Energy Proceedings
Vol 38, 2024
ISSN 2004-2965

Design of Key Parameters of Mooring System and Dynamic Response Analysis for Semisubmersible Wind Turbines

Cheng Zhao[1], Jiawei Chen[2], Xiumin Li[2], Xin Du[2], Lei Wang[1*]

1 College of Automation, Chongqing University, Chongqing, 400044, PR China

2 Goldwind Technology Co., LTD, Wulumuqi, 830000, PR China
(*Corresponding Author: leiwang08@cqu.edu.cn)

ABSTRACT

The harsh operating environment and non-fixed foundation pose a challenge to the power output of the floating wind turbine, so a floating platform for motion within a safe range is required. The paper analyzes the influence of wind-wave coupling, wave direction angle and rotor degree of freedom on the platform movement. It is found that the stability of the floating platform is very sensitive to the key parameters of the mooring system. The mooring system dynamic model is established, and the simulation analysis is carried out by resetting the key parameters of the mooring system. The effects of variables such as the position of the fairlead, the tensile stiffness of the anchor chain, and the mass per unit length of the anchor chain on the platform's motion stability and output power fluctuation are analyzed. It is also of great significance to balance the relationship between the platform's dynamic response and power generation.

Keywords: renewable energy, floating offshore wind turbines, floating platform motion analysis, find and wave loads, mooring system

NONMENCLATURE

Abbreviations	
WT	Wind Turbine
6-DOF	six degrees of freedom

1. INTRODUCTION

Wind energy is a form of renewable and clean energy. Compared to land, the ocean possesses more abundant and stable wind resources. Offshore WTs can be categorized into two types: bottom fixed and floating [4]. Floating offshore WTs have significant cost advantages in deep-water areas located far from land [5]. The aerodynamic performance of the WT plays a crucial role in its ability to capture wind energy efficiently. Compared with the traditional fixed structure WT, the aerodynamic performance of the floating offshore WT is affected by the movement of the additional platform, especially the pitch motion [1]. Liu et al. found that without considering fluid viscosity, the motion of a semi-submersible platform excites resonance response near the natural frequency of the system. Further, by comparing the platform's motion response under parking conditions and operating conditions, it was found that the surge and sway motions were significantly excited at the resonance frequency under stable wind conditions. [2]. Fang et al. studied the aerodynamic characteristics of WTs under pitch motion and demonstrated that the aerodynamic performance of WTs is highly sensitive to the frequency and amplitude of pitch motion. They found that rotor thrust and torque are positively correlated with pitch amplitude, while negatively correlated with pitch frequency. Moreover, when the pitch motion has a low frequency and a high amplitude, the wake interference phenomenon becomes more pronounced [3].

In most studies, researchers have focused on analyzing the platform's motion under wind and wave conditions, with less emphasis on studying the response of various parameters of the WT mooring system. Therefore, this paper firstly analyzes the influence of various factors such as the combined effect of wind and wave, rotor degrees of freedom, and different wave angles on the dynamic response of the platform. Subsequently, the effects of various parameters of the mooring system are introduced to analyze their sensitivity to platform motion responses. In this paper, the research object is OC4-DeepCwind [6], a semi-submersible offshore WT designed by NREL. The study

This is a paper for 15th International Conference on Applied Energy (ICAE2023), Dec. 3-7, 2023, Doha, Qatar.

focuses on the subsequent related work using the seamless interface between FAST and MATLAB Simulink.

2. ANALYSIS OF PLATFORM DYNAMIC RESPONSE CHARACTERISTICS

Different from fixed offshore WTs, floating WTs experience translational and rotational motions under the influence of external loads such as wind, waves, and currents. Each motion can be decomposed into X, Y, and Z directions, resulting in a 6-DOF motion of the platform. The 6-DOF motion includes the displacement of the platform in X, Y, and Z directions known as Surge, Sway, and Heave respectively. It also involves the rotation angle of the platform around the X, Y, and Z axes referred to as Roll, Pitch, and Yaw respectively.

To investigate the dynamic response characteristics of the semi-submersible platform under the combined effect of wind and waves, this paper utilizes the FAST simulation tool and employs a control variate method to analyze the platform's 6-DOF motion in the time domain. The controllable variables considered in this study include wind load, wave load, and rotor degrees of freedom. The incident direction of the waves is taken as the controlled independent variable. Firstly, the paper compares three conditions: wind-wave load coupling, wind load only, and wave load only. In these comparisons, the rotor degrees of freedom are restricted, and the influence of impeller aerodynamics on platform motion is not considered. Only aerodynamic loads other than those from the impeller are considered. Secondly, the study investigates the dynamic response characteristics of the platform by altering the incident direction of waves. This allows for an examination of how different wave directions affect platform motion. Finally, the research explores the influence of rotor degrees of freedom on the dynamic response of the platform.

2.1 Dynamic response simulation and result analysis of the platform under the coupling effect of wind and wave

In the simulation analysis conducted in this section, the wind speed is set to the rated wind speed of 11.4m/s, and the incident direction is aligned with the positive x-axis, indicating that the WT is facing against the wind. The wave spectrum employed is based on the Jonswap spectrum, with a wave height of 5m and an effective period of 10s. Furthermore, the wave direction is set to 0 degrees, meaning that the waves are incident from the positive x-axis direction. In addition, the initial state of the platform is set to the stationary stable state, that is, the initial values of $q_1 - q_6$ are all set to 0. Figures 1-6 present the time domain curves illustrating the 6-DOF motion of the platform under three working conditions: wind and wave load coupling, wind load only, and wave load only. Figure 1 demonstrates that the pitch motion of the platform is significantly influenced by waves, with increased amplitude observed under the combined effect of wind and waves. The roll and yaw motions are predominantly affected by wind, exhibiting noticeable phase differences when subjected to both wind and wave loads. This indicates that the frequency and phase of roll and yaw motions are impacted by the presence of waves. From Figures 4-6, it is evident that the platform's sway motion is significantly influenced by wind, resulting in a delayed phase and reduced amplitude under the combined effect of wind and waves. The pitch and heave motions of the platform are noticeably affected by wave action, with the motion amplitude being higher under the combined action of wind and waves compared to wave-only conditions.

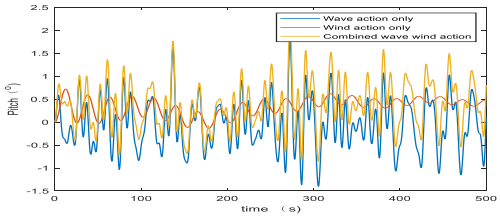

Fig. 1. Pitch motion diagram of platform

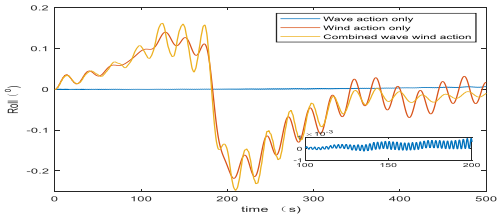

Fig. 2. Roll motion diagram of platform

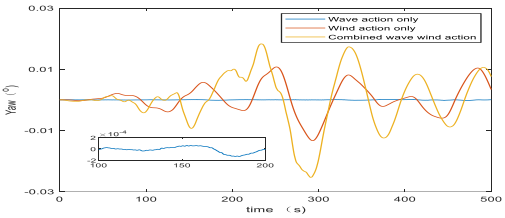

Fig. 3. Yaw motion diagram of platform

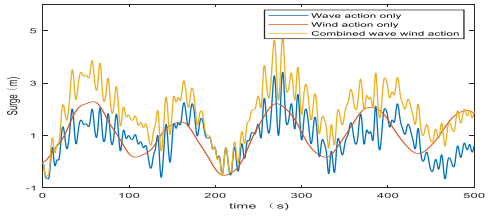

Fig. 4. Surge motion diagram of platform

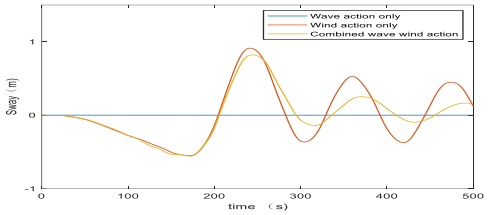

Fig. 5. Sway motion diagram of platform

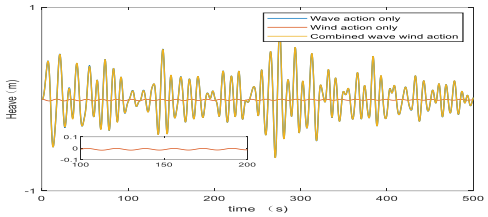

Fig. 6. Heave motion diagram of platform

2.2 Simulation and result analysis of platform dynamic response under different wave directions

The wind parameters are set according to the specifications outlined in Section 2.1. Additionally, the rotor degrees of freedom are restricted, and the incident direction of the waves is divided into seven sea states at equal intervals ranging from 0° to 60°. Figures 7-12 present the time-domain statistical results of the platform's dynamic response under various wave directions. These figures display the maximum, minimum, and average values of the platform's 6-DOF movement during a 500-second runtime. From Figures 7-9, it is evident that as the wave incidence angle increases, the amplitude of the platform's roll motion significantly increases while the pitch motion decreases slightly. The yaw motion is found to be highly sensitive to the direction of wave incidence, with its amplitude reaching a maximum between wave incidence angles of 20o and 30o, followed by a decrease as the wave incidence angle continues to increase. This phenomenon can be attributed to the symmetrical distribution of the three catenaries in the mooring system. As depicted in Figures 10 to 12, an increase in the wave incidence angle results in an increased amplitude of platform sway motion. Additionally, the minimum amplitude of surge motion initially increases and then decreases, while no significant change is observed for heave motion. Furthermore, Figures 7-12 indicate that the mean value of the platform's 6-DOF movement does not exhibit significant changes. This suggests that variations in wave direction angle do not significantly impact the mean value of platform movement.

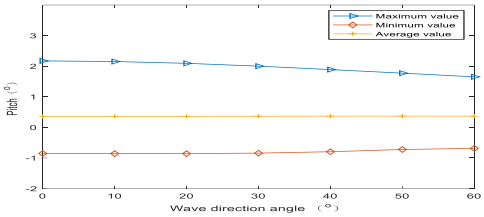

Fig. 7. Time domain statistical results of platform pitch motion at different wave angles

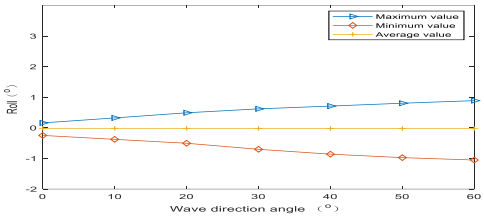

Fig. 8. Time domain statistical results of platform roll motion at different wave angles

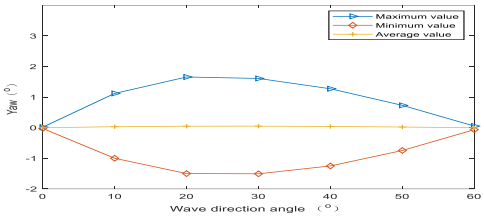

Fig. 9. Time domain statistical results of platform yaw motion at different wave angles

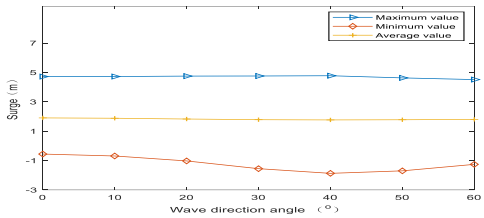

Fig. 10. Time domain statistical results of platform surge motion at different wave angles

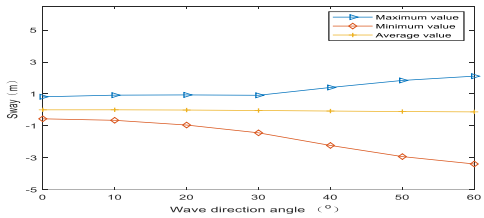

Fig. 11. Time domain statistical results of platform sway motion at different wave angles

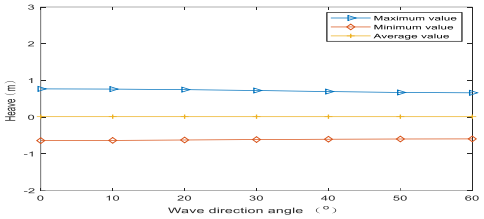

Fig. 12. Time domain statistical results of platform heave motion at different wave angles

2.3 Simulation results and analysis of dynamic response of rotor degrees of freedom to platform

The wind and wave parameters are established based on the specifications outlined in Section 2.1. To control variables, the wave angle is fixed in the positive direction of x. Taking into account the impact of impeller aerodynamic load on the platform's dynamic response, Figures 13-18 present dynamic response curves of the platform with and without rotor degrees of freedom.

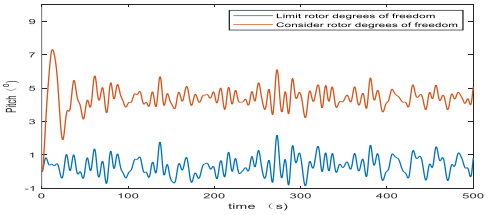

Fig. 13. Platform pitch motion diagram with or without restricted rotor degrees of freedom

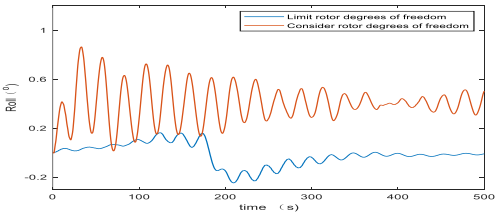

Fig. 14. Platform roll motion diagram with or without restricted rotor degrees of freedom

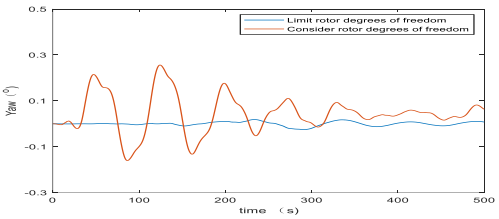

Fig. 15. Platform yaw motion diagram with or without restricted rotor degrees of freedom

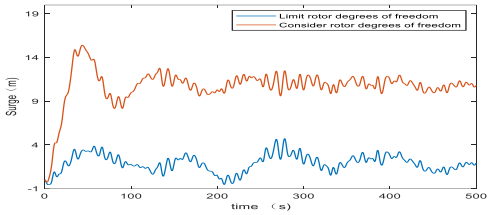

Fig. 16. Platform surge motion diagram with or without restricted rotor degrees of freedom

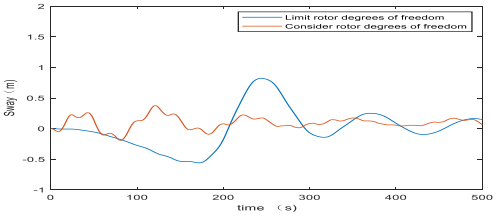

Fig. 17. Platform sway motion diagram with or without restricted rotor degrees of freedom

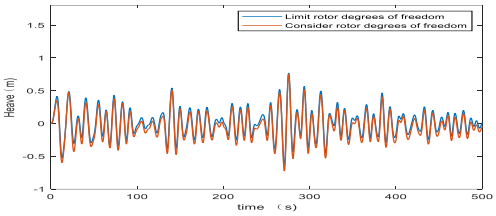

Fig. 18. Platform heave motion diagram with or without restricted rotor degrees of freedom

As observed in Figures 13-15, a strong correlation exists between the rotational motion of the platform and the motion of the rotor. Notably, when considering the degrees of freedom of the rotor, there is a significant increase in the amplitude of pitch motion. This change aligns with what is observed when limiting the rotor degrees of freedom, indicating that the aerodynamic load on the impeller exerted a considerable influence on the pitch motion amplitude. Furthermore, it is worth noting that among all three rotational motions, pitch exhibits a larger amplitude compared to yaw and roll motions. This suggests that pitch motion is more susceptible to external factors and shows greater variability than other rotational motions. Furthermore, noticeable differences can be observed in the phase of roll motion and the mean value of motion when considering or not considering the rotor's degree of freedom. This difference serves as evidence of the coupling effect between rotor motion and wave load. Additionally, Figures 16-18 highlight a clear coupling effect between wave load and rotor motion. The amplitude of surge motion is larger than that of the other two translational motions. Therefore, it becomes crucial

to focus on suppressing pitch and surge movements of the platform during normal unit operation.

3. SENSITIVITY ANALYSIS OF KEY PARAMETERS OF MOORING SYSTEM

The performance of the mooring system plays a crucial role in influencing the dynamic response of the platform. The effectiveness of the mooring system is dependent on various factors, including the distribution mode of the catenaries, the position of the fairlead, and the parameters of the catenaries. For the OC4 semi-submersible WT, the installation position of its fairlead on the foundation column determines the force position exerted on the platform, which has a significant impact on the mooring performance. The catenary force equation is established according to the presence or absence of undercover length, and Figure 19 shows the force of a single anchor catenary.

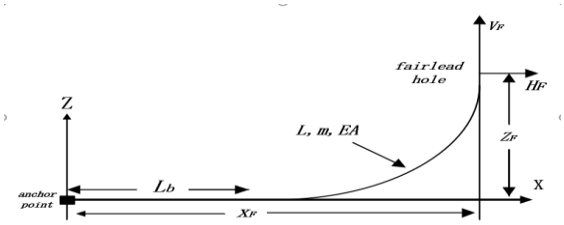

Fig. 19. Diagram of single catenary force

When the catenary is in a relaxed state, the tension at the top of the catenary and the position of the fairlead have a relationship as follows:

$$x_F(H_F,V_F)=L_b-\frac{V_F}{m}+\frac{H_F L_b}{EA}+\frac{H_F}{m}ln\left[\frac{V_F}{H_F}+\sqrt{1+\left(\frac{V_F}{H_F}\right)^2}\right]+\frac{H_F m}{EA}\left(-\left(L_b-\frac{V_F}{m}\right)^2+\left(L_b-\frac{V_F}{m}-\frac{H_F}{C_B m}\right)max\left(L_b-\frac{V_F}{m}-\frac{H_F}{C_B m},0\right)\right) \quad (3\text{-}1)$$

$$z_F(H_F,V_F)=\frac{H_F}{m}\left[\sqrt{1+\left(\frac{V_F}{H_F}\right)^2}-\sqrt{1+\left(\frac{V_F-mL}{H_F}\right)^2}\right]+\frac{1}{EA}\left(V_F L-\frac{mL^2}{2}\right) \quad (3\text{-}2)$$

Where x_F and z_F are the horizontal and vertical positions of the fairlead relative to the anchor point, H_F and V_F represent the horizontal and vertical components of the tension at the top of the catenary, L is the total length of the catenary, m is the mass per unit length of the catenary, EA is the tensile stiffness of the catenary, and C_B is the static friction coefficient between the catenary and the seabed. L_b is the undercover length of the catenary.

When the catenary is in tension, the relationship between the tension at the top of the catenary and the position of the fairlead can be expressed as follows:

$$x_F(H_F,V_F)=\frac{H_F}{m}\left\{ln\left[\frac{V_F}{H_F}+\sqrt{1+\left(\frac{V_F}{H_F}\right)^2}\right]-ln\left[\frac{V_F-mL}{H_F}+\sqrt{1+\left(\frac{V_F-mL}{H_F}\right)^2}\right]\right\}+\frac{H_F L}{EA} \quad (3\text{-}3)$$

$$z_F(H_F,V_F)=\frac{H_F}{m}\left[\sqrt{1+\left(\frac{V_F}{H_F}\right)^2}-\sqrt{1+\left(\frac{V_F-mL}{H_F}\right)^2}\right]+\frac{1}{EA}\left(V_F L-\frac{mL^2}{2}\right) \quad (3\text{-}4)$$

From Equations 1-4, it becomes apparent that the tension at the top of the catenary is directly influenced by factors such as the tensile stiffness of the catenary and the mass per unit length of the catenary. Consequently, it becomes imperative to investigate how variables like fairlead position, anchor chain tensile stiffness, and anchor chain mass per unit length impact mooring performance and platform dynamic response.

3.1 Influence of the position of the fairlead on the motion response of the platform and the tension of the anchor chain

To examine the impact of fairlead position changes on the foundation column and their effect on platform movement response and anchor chain tension, this study focuses on four positions at equal intervals along the length of the 6m foundation column. The water depth at the top is established as 14m. The chosen positions for investigation are -14m, -16m, -18m, and -20m along the z-coordinate axis with no change in the XY coordinates. It is important to note that throughout these positions, a consistent 120-degree symmetric distribution of the catenary is maintained.

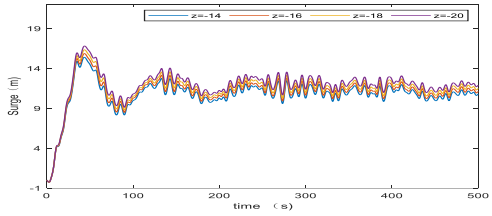

Fig. 20. Platform surge motion diagram of platform under different fairlead positions

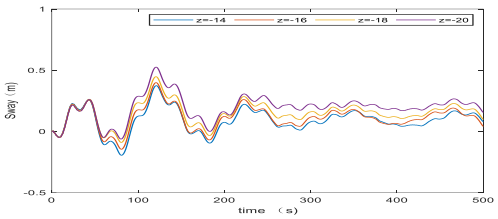

Fig. 21. Platform sway motion diagram of platform under different fairlead positions

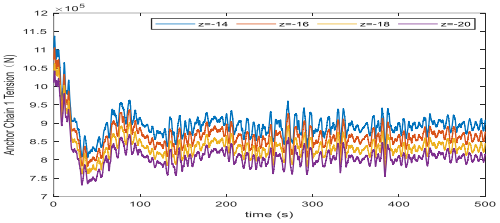

Fig. 22. Tension diagram of anchor chain 1 at different fairlead positions

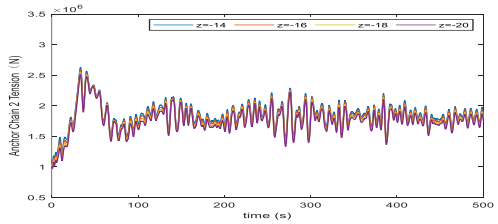

Fig. 23. Tension diagram of anchor chain 2 at different fairlead positions

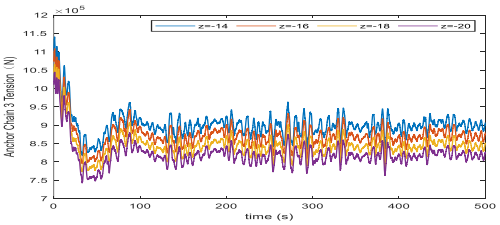

Fig. 24. Tension diagram of anchor chain 3 at different fairlead positions

The 6-DOF movement of the platform during a 500s simulation was analyzed to determine the maximum, minimum, and average values. The results revealed that only the pitch and sway movements of the platform exhibited slight changes, while the rotational movement remained unaffected. It is found that this is because the mooring catenary always maintains a symmetric distribution. The response curves for the pitch and sway motions are shown below. It can be seen from Figure 20-21 that the amplitude of sway and sway increases, indicating that the farther the fairlead is from the top of the foundation column, the more unfavorable the dynamic response of the platform.

The tension variation of the anchor chain is depicted in Figures 22-24. As seen in these figures, when the surge amplitude reaches its maximum, the tension also reaches its maximum due to anchor chain 2 being in a stretching state. Conversely, anchor chains 1 and 3 are in a recovery state during this time, resulting in minimum tension. Upon comparing the tension of the fairlead at four different positions, it becomes apparent that as the fairlead moves farther away from the top of the foundation column, the tension in the anchor chain decreases. This observation highlights the significant impact of fairlead installation position on both platform motion responses and anchor chain loads, with a particular emphasis on anchor chain loads.

3.2 Influence of anchor chain tensile stiffness on platform motion response and anchor chain tension

In order to investigate the influence of anchor chain tensile stiffness on platform motion response and anchor chain tension, this study conducted four numerical simulations with equal intervals of 36.13% of the original value of EA. The remaining parameters of the mooring system were kept constant. The original value of EA in the initial configuration is 5.536E8, and the four cases considered for analysis are referred to as EA1, EA2, EA3, and EA4. These correspond to values of EA set at 3.536E8, 5.536E8, 7.536E8, and 9.536E8 respectively.

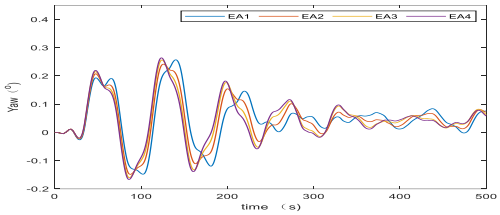

Fig. 25. Platform yaw motion diagram under different anchor chain tensile stiffness

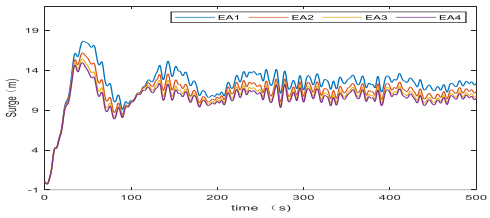

Fig. 26. Platform surge motion diagram under different anchor chain tensile stiffness

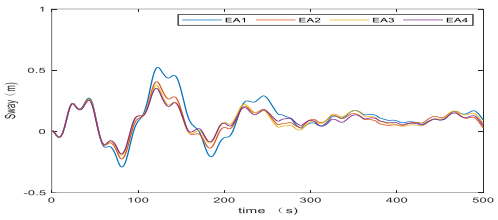

Fig. 27. Platform sway motion diagram under different anchor chain tensile stiffness

The maximum, minimum, and average values of the 6-DOF movement of the platform were calculated during a 500s simulation. It was observed that only the yaw, pitch, and sway movements of the platform exhibited significant changes. The maximum and minimum values for yaw movement were significantly different from the 0 position. The surge movement displayed a reduction in both its maximum value and average value, while the sway movement had values close to the 0 position for both its minimum and maximum values. These findings suggest that an increase in anchor chain tensile stiffness is not favorable for platform yaw movement but can partially dampen surge and sway movements. Figures 25-27 showcase the corresponding time-domain response curves.

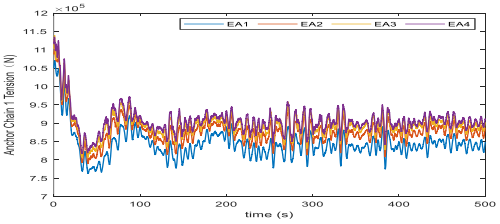

Fig. 28. Tension diagram of anchor chain 1 under different tensile stiffness

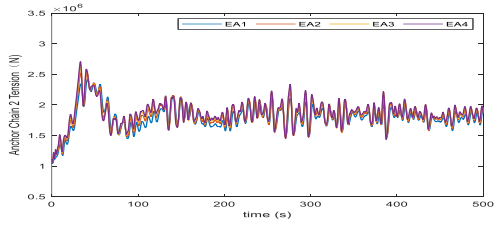

Fig. 29. Tension diagram of anchor chain 2 under different tensile stiffness

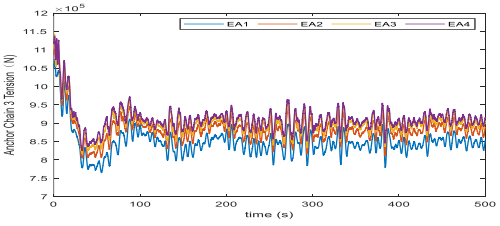

Fig. 30. Tension diagram of anchor chain 3 under different tensile stiffness

The tension variations of the anchor chain are depicted in Figures 28-30. It is evident that the tensile stiffness of the anchor chain has a significant impact on its tension. As the tensile stiffness increases, the tension in the anchor chain also increases substantially, which can have adverse effects on the mooring system. Therefore, it is crucial not to solely pursue high resistance to deformation in the anchor chain for a mooring system. Based on this analysis, it becomes apparent that finding an appropriate balance between suppressing platform motion and reducing mooring loads is essential when selecting anchor chain tensile stiffness.

3.3 Influence of anchor chain mass per unit length on platform motion response and anchor chain tension

In order to investigate the influence of the mass per unit length of the anchor chain on platform motion response and anchor chain tension, this study conducted four numerical simulations at equal intervals of 8.82% of the original value of m. The remaining parameters of the mooring system were kept unchanged. The original value of m in the initial configuration is 113.35, and the four cases considered for analysis are referred to as m1, m2, m3, and m4. These correspond to values of m set at 103.35, 113.35, 123.35, and 133.35 respectively.

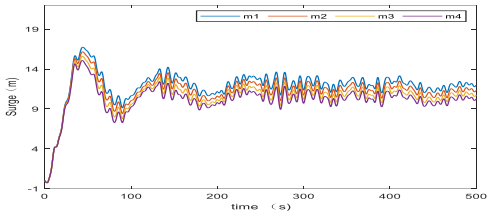

Fig. 31. *Platform surge motion diagram under different anchor chain unit length* mass

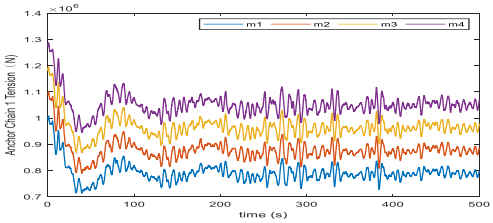

Fig. 32. Tension diagram of anchor chain 1 under different unit length and mass of anchor *chain*

The maximum, minimum, and average values of the 6-DOF movement of the platform were calculated and analyzed during a 500s simulation. It was observed that only the yaw motion of the platform exhibited changes in its rotational movement, while the translational movement also underwent variations. Drawing the motion response curve revealed that under different

mass per unit length of the catenary, both the amplitude and phase of the yaw motion exhibited changes. On the other hand, only the amplitude of the translational motion of the platform showed variations. With an increase in mass per unit length of the catenary, there was a proportional decrease in the amplitude of translational motion. This indicates that the platform's motion is partially inhibited. Plotting the tension curve of the anchor chain reveals that the tension increases in equal proportion with an increase in the mass per unit length of the catenary. Additionally, the changes in translational movement of the platform and the tension of the anchor chain align with those observed in the time domain curve mentioned in section 3.2, with only variations in amplitude. It is once again emphasized that finding a balance between mooring load and platform motion is crucial. Figures 31 and 32 showcase solely the surge motion of the platform and the tension curve of anchor chain 1.

4. CONCLUSIONS

In this paper, the NERL-5MW semi-submerged offshore WT is selected as the research subject. The 6-DOF motion response of the platform under different operating conditions is calculated using the control variable method and the FAST simulation software. When analyzing the motion response of the platform under the combined influence of wind and waves, it becomes evident that the motion of the platform is significantly influenced by wave action. Additionally, wind action leads to an increase in the amplitude of the platform's motion. When examining the motion response of the platform under varying wave direction angles, it becomes apparent that the yaw motion is highly sensitive to the incident direction of the waves. Furthermore, the platform's motion response is influenced by the distribution mode of the three catenaries in the mooring system. Considering the impact of rotor rotation on the dynamic response of the platform, a close relationship between rotational motion and rotor motion is observed. The rotation of the rotor significantly affects the amplitude of pitch motion. Additionally, both pitch and surge motions exhibit larger amplitudes compared to other movements.

Considering that the performance of the mooring system is influenced by various parameters of the catenary, this paper also investigated the effects of three factors: the position of the fairlead, the tensile stiffness of the anchor chain, and the mass per unit length of the anchor chain on both mooring performance and platform dynamic response. It was discovered that there exists a contradictory relationship between mooring load and platform motion. Therefore, in normal operating conditions of the unit, it is crucial to prioritize the consideration of pitch and surge motion of the platform. It is important to strike a balance between mooring load and platform dynamic response, as this has significant implications for ensuring stability in the platform's motion.

ACKNOWLEDGEMENT

This work was supported by the National Natural Science Foundation of China (NO.51875058), Central University Frontier Discipline Special Project (NO. 20 19CDQYZDH025).

REFERENCE

[1] Fang Y, Duan L, Han Z, et al. Numerical analysis of aerodynamic performance of a floating offshore wind turbine under pitch motion. Energy, 2020, 192:628-635.
[2] Liu Y, Hu C, Sueyoshi M, et al. Motion response characteristics of a Kyushu-University semi-submersible Floating Wind Turbine with trussed slender structures: Experiment vs. numerical simulation. Ocean Engineering, 2021, 232:1212-1227.
[3] Fang Y, Duan L, Han Z, et al. Numerical analysis of aerodynamic performance of a floating offshore wind turbine under pitch motion. Energy, 2020, 192:628-635.
[4] Zhen L, Minmin Y, Decai H, et al. Research on the Development of Offshore Wind Power. Ship Engineering, 2020, 42(8):20-25.
[5] Xu B. Current Status and Prospects of Offshore Wind Power Development in China. Ship Engineering, 2021, 43(10):1-4.
[6] Robertson A, Jonkman J, Masciola M, et al. Definition of the Semisubmersible Floating System for Phase II of OC4. Scitech Connect Definition of the Floating System for Phase IV of Oc3, 2014.